

Characterization of anionic and cationic functionalized bacterial cellulose nanofibres for controlled release applications

Marko Spaic · Darcy P. Small · Justin R. Cook ·
Wankei Wan

Received: 9 May 2013 / Accepted: 20 January 2014 / Published online: 7 February 2014
© Springer Science+Business Media Dordrecht 2014

Abstract Bacterial cellulose (BC) is a biocompatible biopolymer synthesized by *Gluconacetobacter xylinus*. In this study, BC was oxidized and aminated to produce hydrogels for biomedical applications, and the products were characterized. A carboxyl (pK_a of 3.9 ± 0.1) content of 1.13 ± 0.02 mmol/g was obtained with the TEMPO-catalyzed oxidation. Epichlorohydrin-mediated amination introduced amine groups (pK_a of 11.0 ± 0.1) up to 1.74 ± 0.06 mmol/g. The oxidation of BC caused a decrease in its ζ -potential to -103 ± 6 mV, and amination increased the ζ -potential to -4 ± 6 mV. The fibre diameter decreased after both reactions. The high absolute value of the ζ -potential for oxidized BC led to superior colloidal stability in water, and a 390 % increase in water retention. The oxidized BC hydrogel was also found to increase in water retention fivefold from pH 1 to 7, making it a smart hydrogel. The cationic and anionic BC hydrogels described here could be used for several biomedical applications, including self-assembling drug delivery devices.

Keywords Bacterial cellulose · Polyelectrolyte polymers · Hydrogel swelling · Controlled drug release

Introduction

Bacterial cellulose (BC) is a biopolymer of β -1-4-linked glucopyranose molecules, produced at a high yield by the gram-negative, acetic acid bacteria *Gluconacetobacter xylinum* (Iguchi et al. 2000). These bacteria produce BC with an average degree of polymerization (D_{pn}) of 2,000–8,000 (Klemm et al. 2005). Although BC is chemically identical to plant cellulose (PC), BC is produced without hemicellulose and lignin, which need to be removed during purification of PC, reducing its D_{pn} below that of BC (Ross et al. 1991). BC's fibre diameter of ~ 30 nm is two orders of magnitude smaller than that of PC, giving it a much larger surface area per unit mass, which contributes to its high equilibrium water content (EWC) of up to 99 %. Nanocrystalline cellulose (NCC) can be produced from both PC and BC by acid hydrolysis (Habibi et al. 2010). BC has been investigated for use in numerous biomedical applications (Czaja et al. 2006), including as a wound dressing (Solway et al. 2011), and a drug delivery device (Czaja et al. 2007). BC has also served as a scaffold material for tissue regeneration (Svensson et al. 2005), in composites with hydroxyapatite (HA) to restore bone defects (Saska et al. 2011; Wan et al.

M. Spaic · J. R. Cook · W. Wan
Biomedical Engineering Graduate Program, The
University of Western Ontario, London, ON, Canada

D. P. Small · W. Wan (✉)
Department of Chemical and Biochemical Engineering,
University of Western Ontario, London, ON N6A5B9,
Canada
e-mail: wkwan@uwo.ca

2006), and in composites with poly (vinyl alcohol) for vascular prostheses (Millon et al. 2008).

The use of BC for many applications necessitates its surface functionalization to form anionic and cationic polyelectrolytes (PE), specifically through carboxylation (oxidation) and amination. Oxidized cellulose derived from cotton linters has been used to create a sustained-release drug delivery systems by loading the model cationic drug phenylpropanolamine hydrochloride through ionic bonding (Zhu et al. 2004a, b). When the same drug was linked to oxidized PC by a covalent amide bond, its controlled release was sustained for several days (Zhu et al. 2001). Due to its high negative charge density, oxidized cellulose can also be used to immobilize proteins (Kumar and Deshpande 2001) and antibiotics (Zimnitsky et al. 2006). Similarly, cationic polymers have been used to bind and deliver DNA and RNA with the additional advantage that they are less immunogenic than viral vectors (Merdan et al. 2002; De Smedt et al. 2000). PE show strong affinity to inorganic materials through ionic bonding (Wilson et al. 1983), making anionic or cationic BC derivatives potentially useful in nanocomposites with HA for bone tissue engineering. Under the right conditions, anionic and cationic PE can self-assemble into alternating molecule-thick layers (Decher 1997), colloidal particles (Sukhorukov et al. 1998), micelles (Weaver et al. 2003), or templated nanostructures (Wang and Mohwald 2004), which could be useful for controlled drug release and targeted drug delivery.

Conversion of BC to a PE introduces a surface charge, which varies with pH, and, depending on the state of protonation/deprotonation, influences the Zeta potential (ζ -potential) of the nanofibres (Berg et al. 2009). The surface charge in turn affects cell attachment and cellular uptake of nanoparticles, because a favourable electrostatic interaction greatly promotes both (Kumar et al. 2008; Kim et al. 2009). By knowing how surface charge resulting from oxidation and amination reactions affects BC's ζ -potential, it will be possible to predict the modified BC's cellular uptake for drug delivery as a function of pH. By introducing acidic and basic groups to the BC surface, it may also be possible to create pH and ionic strength-responsive swelling hydrogels, allowing for controlled drug release after an appropriate change in conditions.

Although oxidized cellulose originated from a variety of cellulose sources has been characterized (Saito and Isogai 2004; Saito et al. 2007, 2006b; Okita et al. 2010; Isogai et al. 2011), little systematic work has been performed on the BC-derived product (Ifuku et al. 2009), and even less on the aminated BC product. A detailed examination of functionalized BC is necessary before it can be used for medical applications where it is superior to PC because of the aforementioned properties (Czaja et al. 2006). The goal of this work is to systematically characterize these BC derivatives, including the determination of their pK_a values, degree of substitution, and ζ -potentials, which are important parameters for the design of drug delivery and controlled release systems. The BC-derived hydrogels produced were then shown to be pH responsive, which may allow for triggered drug release in drug delivery and other biomedical applications.

Experimental

Chemicals

All chemicals were ACS reagent grade and purchased from Sigma-Aldrich (St. Louis, MO, USA).

BC growth and harvest

Gluconacetobacter xylinus (BPR 2001) bacteria were cultivated in a static medium consisting of 0.22 M fructose, 26.63 mM ammonium sulphate, 7.34 mM potassium phosphate monobasic, 1.01 mM magnesium sulphate heptahydrate, 14.28 mM tri-sodium citrate, 45.80 mM citric acid and 5 g/l yeast extracts. After 3 weeks of growth at room temperature in 500 ml Erlenmeyer flasks, the pellets were blended with a Waring Commercial Laboratory Blender (model 51BL30, Torrington, CT, USA) and purified by washing with 1 % sodium hydroxide at 90 °C for 1 h, and then repeatedly with distilled water.

BC functionalization

Oxidation

0.1 g (dry weight) sample of never-dried BC was suspended in an 80 ml solution containing 1.2 mM

2,2,6,6-tetramethylpiperidine-1-oxyl (TEMPO) and 12 mM sodium bromide. 10 mmol/g BC of sodium hypochlorite was added to begin the oxidation reaction (Saito and Isogai 2004). The pH was maintained at 10.5 by adding 0.5 M sodium hydroxide when necessary. After 4 h, the reaction was quenched by adding 2 ml of ethanol. Repeated washes were performed with distilled water by centrifugation with the Sorvall Refrigerated Super-speed Centrifuge (model RC-5B, Asheville, NC, USA) at 10,000 rpm, until the oxidized BC reached the pH of the distilled water.

Amination

0.1 g sample of BC was placed in 40 ml of 1 M sodium hydroxide solution and stirred until the contents were well dispersed. The mixture was heated to 60 °C with constant stirring. Once the desired temperature was reached, 18 mmol epichlorohydrin per gram of BC was added, and allowed to react at 60 °C for 2 h (Dong and Roman 2007). The solution was cleaned with distilled water by centrifugation until the pH was below 12. The 0.1 g of BC was resuspended in 40 ml 0.01 M sodium hydroxide, and 1.5 ml of ammonium hydroxide (29.4 % w/v) was added to the pH 12 solution. The mixture was then left to stir at 60 °C for an additional 2 h to produce the amine functionality. The product was washed and centrifuged until the pH was reduced to 7, after which it was stored at 4 °C.

Acid/base titration

Oxidized BC and aminated BC

To quantify the amount of carboxyl groups, 0.1 g of never-dried oxidized BC was suspended in 35 ml of aqueous hydrochloric acid solution of pH 3. This solution was titrated against 1 mM sodium hydroxide up to pH 7. The difference in the number of moles of acid between the oxidized BC and BC was considered to be the number of moles of carboxylic acid functional group introduced to the oxidized BC surface, and their pK_a was determined from the titration curve as the pH halfway to the equivalence point.

$$\text{Carboxyl Content} \left(\frac{\text{mmol}}{\text{g Oxidized BC}} \right) = \frac{\left(\frac{\text{Oxidized BC} - \text{Control BC (volume of 0.1 M NaOH to Neutralize)}}{1000} \right)}{\text{Mass of Oxidized BC}} \quad (1)$$

$$\text{Amine Content} \left(\frac{\text{mmol}}{\text{g Amine BC}} \right) = \frac{\left(\frac{\text{Amine BC} - \text{Control BC (volume of 0.01 M HCl to Neutralize)}}{1000} \right)}{\text{Mass of Amine BC}} \quad (2)$$

A similar procedure was used to determine the amine content and pK_a of the aminated BC, except the titration was started in a solution of aqueous sodium hydroxide of pH 13, and titrated down to pH 8.

X-ray diffraction (XRD)

Dried films of BC, oxidized BC and aminated BC were cut and several pieces were spread in random orientation over Beta Diamond Products 27 × 46 mm Frosted Petrographic Slides (Yorba Linda, CA). The Rigaku-Rotaflex diffractometer (model RU-200BH) with a Co-K α radiation ($\lambda = 1.79 \text{ \AA}$) was used to record the XRD patterns at 30 kV and 44 mA. Spectra with a 2 θ diffraction angle were scanned from 0.0° to 90.0°, with a 0.2° step size. The D-spacing (spacing between similar crystal planes) was determined by analysing the peaks after fitting the diffraction patterns with the Pearson VII function (Prevey 1986). Scherrer's equation (Patterson 1939) was used to calculate the average crystallite size. The crystal spacing in the amorphous region was estimated from the position of the maximum of the amorphous halo (Klug and Alexander 1974). The Herman and Weidinger method (Benedetti et al. 1983) was used to determine the degree of crystallinity.

Transmission electron microscopy (TEM)

The morphology of plain BC, oxidized BC, and aminated BC fibres was analyzed with the TEM method. Suspensions of BC and functionalized BC (1 g/l wet weight) were sonicated for 5 min at 60 W using the Misonix XL-2000 sonication probe (Newtown, CT, USA). One drop (~100 μ l) of suspension was added to Formvar carbon-coated 100 mesh

copper grids (Electron Microscopy Sciences, Hatfield, PA, USA), allowed to settle for 3 min, and excess liquid was dabbed off onto filter paper. Post-staining was done with either 2 % w/v uranyl acetate or 2 % w/v phosphotungstic acid for 3 min. Imaging was conducted using a Philips CM-10 TEM (New York, NY, USA) set at an accelerating voltage of 80 kV with images captured using a Hamamatsu digital camera. Fibre diameters were determined manually using ImageJ (1.43U Java 1.6.0_10 32 bit, Wayne Rasband, National Institute of Health, Bethesda, MD, USA).

ζ-Potential

0.1 mg wet weight of BC, oxidized BC and aminated BC were suspended in 10 ml of deionised water and sonicated for 30 min with the VWR Ultrasonic Cleaner (model B2500A-MTH, West Chester, PA) with the output of 85 W, 42 kHz. The ζ-potentials of the homogenous dispersions were measured with the Zetasizer 3000HSa (model DS5301, Malvern Instruments, UK). Peak analysis for the ζ-potential plots was performed using the Zetasizer software PCS V.1.4 (Malvern Instruments, UK).

Water retention value (WRV)

Samples of never-dried plain BC, oxidized BC and aminated BC were suspended in solutions with pH values of 7, 1–10 and 4–13, respectively. The samples were centrifuged at 10,000 rpm at room temperature for 10 min, and their wet weights (W_w) were recorded. The samples were then dried in the vacuum oven overnight at 60 °C and their dry weights (D_w) were measured. The water retention values (WRVs) were calculated with the following equation (Saito and Isogai 2004):

$$WRV (\%) = \frac{W_w - D_w}{D_w} \times 100 \quad (3)$$

Statistics

Statistical analysis was performed with SigmaStat v.3.5 for Windows (Systat Software, San Jose, CA, USA). The mean values of all parameters were reported ± 1 standard error. Individual comparisons to the control were performed with an unpaired t test and multiple comparisons were performed with a one-

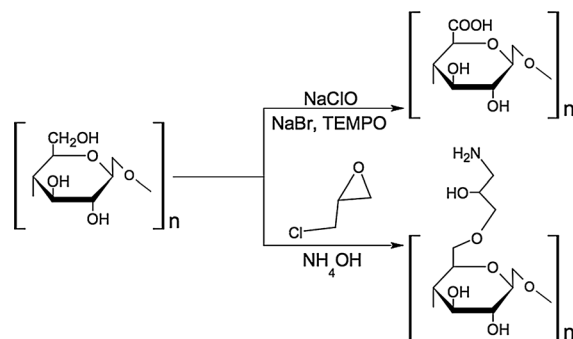


Fig. 1 A schematic summarizing the reactions used to produce the BC derivatives

way ANOVA with a Tukey's Post Hoc Test, and a value of $P \leq 0.05$ was considered significant.

Results and discussion

To create an anionic BC derivative, we selectively oxidized the primary alcohol groups of cellulose to carboxylic acids using the stable nitroxyl radical TEMPO and sodium bromide as catalysts, while sodium hypochlorite was the primary oxidant (Fig. 1) (de Nooy et al. 1995; Saito and Isogai 2004). The chemical structure of this product has been well characterized in the literature, and the oxidation reaction has been found to result in the selective conversion of the primary alcohol groups (at carbon six) of anhydroglucose residues to carboxylic acids (Saito et al. 2005; Lasseguette 2008).

To create a cationic BC derivative, primary amine groups were introduced by functionalizing the surface of BC with epoxy groups through the epichlorohydrin-mediated reaction, followed by ring opening with ammonium hydroxide (Dong and Roman 2007). Although it is not known to be selective for the primary alcohol, this reaction scheme has been shown to decorate cellulose with a primary amine group, and has been used for various applications, including fluorescence labeling (Dong and Roman 2007; Mahmoud et al. 2010).

By titrating oxidized BC with sodium hydroxide solution, it was determined that the carboxylate group had a pK_a of 3.9 ± 0.1 (Table 1). The pK_a of the amine group of aminated BC was found to be 11.0 ± 0.1 . The carboxyl content of 1.13 ± 0.02 mmol/g determined for oxidized BC corresponds to 18.9 ± 0.3 % of the

Table 1 Summary of substituent content and pK_a of oxidized BC and aminated BC

	Substituent group content (mmol/g)	pK_a of substituent group
Oxidized BC	1.13 ± 0.02	3.9 ± 0.1
Aminated BC	1.74 ± 0.06	11.0 ± 0.1

Substituent group content values are shown ± 1 standard error ($n = 3$)

primary hydroxide groups (at carbon six) being oxidized, or 1 per 5.2 ± 0.1 anhydroglucose units. The degree of functionalization was higher for amination, calculated at 1.74 ± 0.06 mmol/g. Fukuzumi et al. (2010) stated that the pK_a value of the C6 carboxyl group of TEMPO-oxidized regenerated cellulose was approximately 3.6 (Fukuzumi et al. 2010). Zhu et al. (2004a) found that the pK_a of oxidized cellulose derived from cotton linters was 4.0 (Zhu et al. 2004a). Kötz et al. (1990) on the other hand reported the pK_a of oxidized cellulose of plant origin to be lower, at 2.8 (Kötz et al. 1990). However, their lower pK_a value can be explained by the higher ionic strength (the polymer was titrated in a 1.0 M sodium chloride solution), since the pK_a of carboxylic acids decreases with increasing ionic strength.

By using the Henderson–Hasselbalch equation (Po and Senozan 2001), it can be calculated that the carboxyl group, with its pK_a of 3.9 ± 0.1 , will be over 99 % deprotonated at pH 7.4. Therefore, the carboxyl group of oxidized BC is negatively charged at physiological pH, and thus is a good candidate for ionic complex formation with cationic molecules, such as the anticancer drug doxorubicin (pK_a 8.3), among other cationic drugs.

In contrast to oxidized BC, the pK_a value of aminated BC was 11.0 ± 0.1 . This indicates that the aminated BC would be a good candidate for gene delivery, as the amine groups would be protonated at physiological pH, and be able to form an ionic complex with DNA, RNA, and negatively charged proteins (De Smedt et al. 2000). Relative to other amine derivatives in the literature, the basicity of aminated BC is high. One study measured the protonation behaviour of 6-deoxy-6-(2-aminoethyl)amino cellulose (DAEAC) via potentiometric titrations, a compound containing a primary amine group attached to a functional group bound to the C6

of cellulose. DAEAC was found here to have a pK_a of 9.1, a value that increased to 9.5 with increasing ionic strength conditions (Zemljic et al. 2011). In other studies, primary amine-containing chitosan had a pK_a of only 6.5 (De Smedt et al. 2000), and a tertiary polyelectrolyte amine derivative was found to have a pK_a of 9.5 (Liesiene 2010). However, ethylamine contains a similar primary amine and has a similar pK_a of 10.7.

The limited oxidation level of BC (below 20 %) can be ascribed to the low accessibility of the reagents to the anhydroglucose units buried in the crystalline regions of cellulose I, as the TEMPO-mediated oxidation preferentially targets hydroxyl groups exposed on the surface of the fibres (Okita et al. 2010). The hydrogen bonding within the crystalline regions greatly decrease the accessibility of the primary hydroxyl groups, thus the majority of the primary hydroxyl groups of oxidized BC remain unreacted. Okita et al. (2010) similarly deduced that total introduction of carboxyl groups can vary 0.5–1.7 mmol/g for various sources of PC, including softwood, hardwood and cotton. While it is known that the TEMPO-mediated oxidation is regioselective for the primary alcohol group of glucose units due to the steric hindrance caused by the four methyl groups of TEMPO (de Nooy et al. 1995), in contrast to TEMPO oxidation, the epichlorohydrin-mediated amination reaction can occur at any hydroxyl group in cellulose.

XRD was used to study the changes in crystallinity, crystal size and spacing following an oxidation or amination reaction of BC, to determine the effect that these reactions have on the crystal structure of BC. All of the diffraction patterns from Fig. 2 are in close agreement with those reported in literature for cellulose I from plant sources (Wada et al. 1997). It is apparent that significant peak shifting or the appearance of new peaks is not observed in the XRD pattern following functionalization, providing evidence that introduction of new groups to BC fibres occurred on the crystal surfaces and in the amorphous regions.

The first diffraction peak in Fig. 2, at 17° , corresponds to the (1 0 0) plane of cellulose I_α and the (1 $\bar{1}$ 0) plane of I_β , whereas the second diffraction peak, at 19° , corresponds to the (0 1 0) plane I_α and the (1 1 0) plane of I_β (Wada et al. 1997). The third diffraction peak, at 26° , corresponds to the (1 1 0) plane of cellulose I_α and the (2 0 0) plane of I_β . The

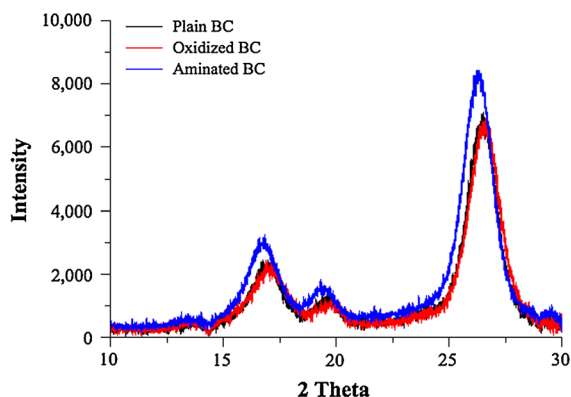


Fig. 2 XRD patterns of plain BC, oxidized BC, and aminated BC

three diffraction peaks for cellulose I had previously been characterized to have respective D-spacing values of 0.614, 0.532 and 0.394 nm (Wada et al. 1997), agreeing with what are reported in Table 2 below.

From Table 2 it can be seen that there is a slight increase in crystallinity following oxidation of BC. This was expected since degradation of BC to celluronic acids in the amorphous regions would occur during the oxidation reaction, leading to their loss in the water-soluble fraction, thus increasing the overall crystallinity percentage. A periodate oxidation was also found to increase the crystallinity of cotton in the literature (Yun and Chen 2011). Another study found that the crystallinity was nearly unchanged for cotton linter (remained about 85 %), and slightly increased for low-crystalline cellulose I (65–75 %) following the TEMPO-mediated oxidation. This is comparable to the approximate crystallinity change of 69–75 % reported here for oxidized BC using the same oxidizing agent.

Saito and Isogai (2004) postulated that the increase in crystallinity can be explained by a partial loss of the amorphous regions during the washing process due to their increase in water-solubility (Saito and Isogai 2004). Although further tests are required, it is plausible that the increase in crystallinity of aminated BC can be similarly explained by a partial loss of the amorphous region in the water-soluble fraction following introduction of charge.

The degradation to soluble products and loss of the amorphous regions can also explain the decrease in inter-crystal distance that was observed, representing the loss of amorphous region between the crystal structures. The greater increase in crystallinity following the oxidation reaction than the amination is explained by a greater decrease in crystal spacing. The D-spacing, representing the spacing between similar crystal planes, does not change following the reactions, due to these reactions occurring on the crystal surface. Lastly, the crystal size (crystal structure) decreased, possibly due to the reaction at the crystal surface causing some of the oxidized chains to disperse or fold off the crystal, and become non-crystalline due to a change of the hydrogen bonding with water.

To study the effects of functionalization on the morphology of the fibres, 0.1 g/l suspensions of sonicated BC fibres were dried on formvar-coated TEM grids and observed with transmission electron microscopy (Fig. 3).

As the electron microphotographs in Fig. 3 show, the oxidized and aminated BC fibres exhibit partial debundling of fibrils from the ordered bundles that make up the bigger fibres in unmodified BC. To more accurately analyze the morphology of fibres in the

Table 2 A summary of crystallinity parameters obtained from the XRD patterns for plain BC, oxidized BC and aminated BC

	Crystallinity (%)		D-spacing (nm)	Crystal size (nm)	Inter-crystal distance (nm)
Plain BC	69 ± 1 ^a	2θ = 17°	0.61 ± 0.01 ^a	5.13 ± 0.02 ^a	6.4 ± 0.1 ^a
Oxidized BC	75 ± 1 ^b		0.61 ± 0.01 ^a	4.37 ± 0.03 ^b	5.4 ± 0.1 ^b
Aminated BC	73 ± 1 ^b		0.61 ± 0.01 ^a	4.67 ± 0.02 ^c	6.0 ± 0.1 ^c
Plain BC		2θ = 19°	0.53 ± 0.01 ^a	5.6 ± 0.1 ^a	6.9 ± 0.2 ^a
Oxidized BC			0.53 ± 0.01 ^a	4.3 ± 0.1 ^b	5.3 ± 0.3 ^b
Aminated BC			0.53 ± 0.01 ^a	5.1 ± 0.1 ^c	6.2 ± 0.1 ^c
Plain BC		2θ = 26°	0.39 ± 0.01 ^a	7.17 ± 0.04 ^a	8.7 ± 0.1 ^a
Oxidized BC			0.39 ± 0.01 ^a	7.00 ± 0.06 ^a	8.1 ± 0.1 ^b
Aminated BC			0.39 ± 0.01 ^a	7.00 ± 0.07 ^a	8.3 ± 0.2 ^{ab}

Values are shown ± one standard error, and significantly different parameters are marked with different letter superscripts (n = 3)

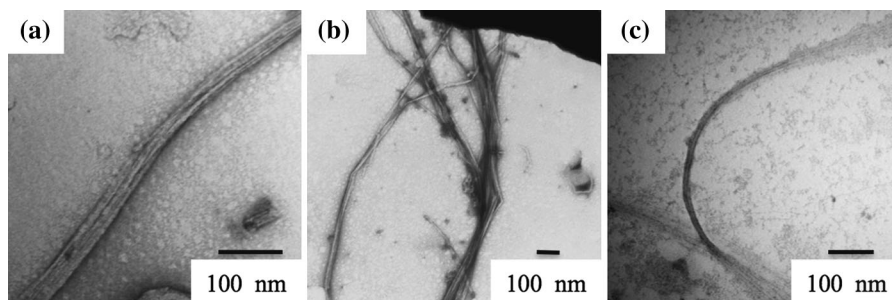


Fig. 3 TEM images of **a** plain BC, **b** oxidized BC, and **c** aminated BC samples

TEM images, their diameters were measured. It is expected that the diameter of BC would decrease following the TEMPO-mediated oxidation and amination with the epichlorohydrin reaction, since these reactions introduce new functional groups to the fibril surface, disrupting the hydrogen bonds between fibrils which bundle them into fibres (Fig. 3). The repulsion due to ionic charge on the surface of the fibres leads to partial disintegration, and thus formation and stabilization of fibres of smaller diameter. Since the degree of functionalization is higher for aminated BC, we would expect even more splitting or fraying of fibres. Indeed, as indicated in Fig. 4, the average diameter of BC fibres measured did decrease by a statistically significant amount ($P \leq 0.05$) following the oxidation and amination reactions, with the latter producing the smallest average fibre diameters of 13.6 ± 0.4 nm.

The average diameter of oxidized BC fibres (16.7 ± 0.4 nm) indicated that not all the fibres were broken up to fibrils, but many remained in bundles of fibrils that make up the larger cellulose fibre. Conversely, Saito et al. (2006a, b) illustrated with electron microscopy that a homogeneous dispersion of individualized cellulose fibrils (3–5 nm in width) can be obtained with the TEMPO-mediated oxidation of celluloses (Saito et al. 2006a). A fibril is the smallest element in the cellulose structure hierarchy after the individual glucan chains and subfibrils, and is 3–5 nm in diameter. The discrepancy with our results can be explained by the fact that the samples in this study were not pre-treated by blending, mercerization or other methods. These pre-treatment methods disrupt crystallinity and cause a homogeneous dispersion of oxidized cellulose fibres, and can explain the difference between our results and what has been previously reported.

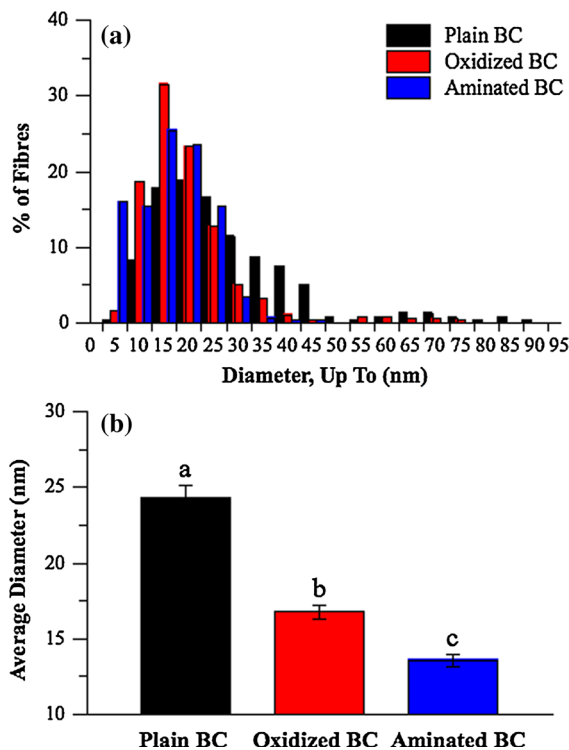


Fig. 4 **a** Size distributions and **b** average diameters of over 300 plain BC, oxidized BC and aminated BC fibres measured from TEM images. Average diameter values are shown ± 1 standard error and significantly different values ($P \leq 0.05$) between plain BC, oxidized BC, and aminated BC are marked with different letters

To evaluate how surface oxidation of BC affects the charge of BC fibres, ζ -potential measurements were performed on fibre suspensions at pH 7. Figure 5a shows that BC has a ζ -potential of -42 ± 7 mV, where the ζ -potential of BC upon oxidation was decreased to -103 ± 6 mV due to the negative charge of the carboxyl groups, while the positive

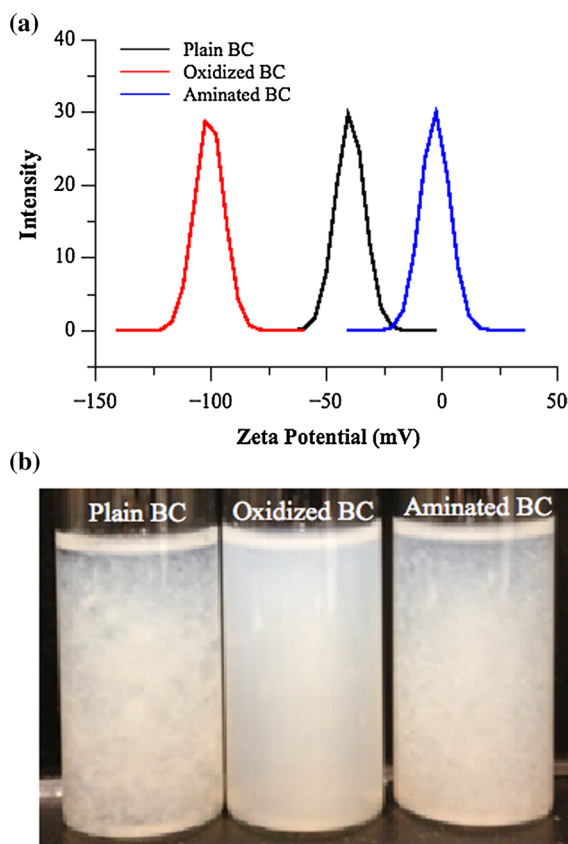


Fig. 5 **a** ζ -Potential measurement of sonicated dispersions of plain BC, oxidized BC and aminated BC at pH 7. **b** Photographs of sonicated dispersions of plain BC, oxidized BC and aminated BC at pH 7

charge introduced by amination caused it to increase to -4 ± 6 mV.

The ζ -potential of PC has been extensively studied, and it has been found that sources such as cotton have a low negative value of between -10 and -20 mV in water at neutral pH (Bellmann et al. 2004). However, it has also been reported that the magnitude of the negative ζ -potential can vary greatly with water content of the fibres, salt concentration and formation of a double layer (Bellmann et al. 2004; Lee et al. 2011; Lokhande and Salvi 1978). The negative value of -42 ± 7 mV for plain BC obtained in Fig. 5a could be attributed to one or more of these factors although there is no definitive explanation offered in the literature cited.

It has been previously shown that the ζ -potential of PC can be modified by oxidation, due to the negative charge brought on by the introduction of the anionic carboxylate groups. Okita et al. (2010) compared the

ζ -potentials of oxidized celluloses of different plant origins produced by the TEMPO-mediated reaction. They found that although their carboxyl contents varied, the oxidized celluloses all had very similar ζ -potentials, around -75 mV, higher than the one of oxidized BC reported in this study (-103 ± 6 mV). Although the ζ -potential of aminated BC has not been measured in the literature, it has been shown that cationic surface modification of cellulose can cause a reversal in surface charge from negative to positive. Mahmoud et al. (2010) found that their flax fibre cellulose-derived NCC had a ζ -potential value of -31.3 mV at pH 7 (Mahmoud et al. 2010). Covalent binding of a cationic, amine-containing dye rhodamine B isothiocyanate (RBITC) lead to reversal of ζ -potential, to a positive value of 8.7 mV at the same pH. This is in line with the charge increase from -42 ± 7 to -4 ± 6 mV upon amination reported here. Moreover, they found the values were pH-dependent, where the ζ -potential of the RBITC-labelled NCC became more positive at a lower pH, indicating the protonation of amine groups.

Previous work has shown that cationic plant NCC fibres can penetrate the cell membrane, while the anionic fibres form aggregates around the cell but do not penetrate its membrane under physiological pH conditions due to repulsive forces (Mahmoud et al. 2010). With the amination reaction and the carboxylation reactions presented here, it should be possible to increase the ζ -potential of BC by the attachment of cationic species, therefore making it possible for cellular uptake by mammalian cells, a property that would be desirable for cationic drug delivery applications.

Figure 5b shows the photographs of the dispersions of freshly sonicated plain BC, oxidized BC, and aminated BC fibres. As one would predict from the ζ -potentials shown in Fig. 5a, oxidized BC, with its highly negative ζ -potential, forms an excellent dispersion, while plain BC and aminated BC, with their lower ζ -potential, form poor dispersions. The high value of the ζ -potential for oxidized BC increases its colloidal stability through electrostatic repulsion.

Although the effect of the surface reactions on turbidity was not directly investigated in this report, it was obvious on visual inspection that dilute solutions of oxidized BC were more transparent than dilute solutions of BC or aminated BC. Similarly, Saito et al. (2007) found that the carboxyl content caused an improvement in the dispersion behaviour of oxidized

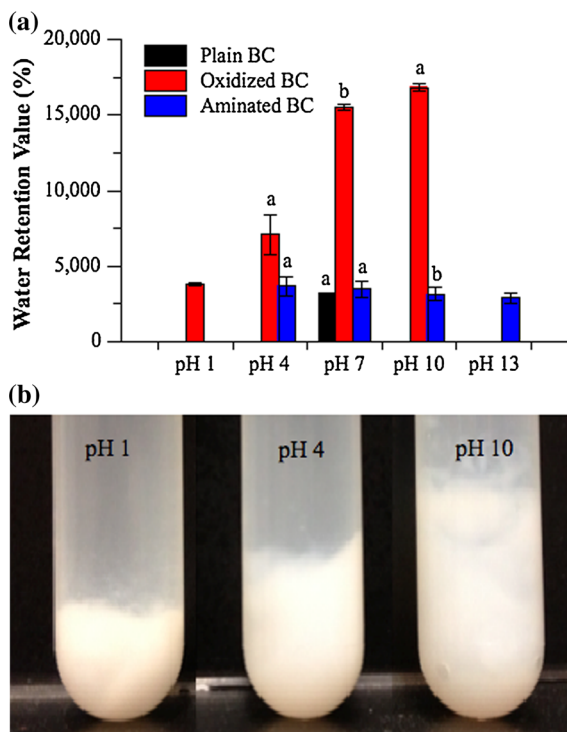


Fig. 6 **a** WRVs of plain BC at pH 7, oxidized BC from pH 1 to 10, and aminated BC from pH 4 to 13. WRVs are shown ± 1 standard error and significantly different values ($P \leq 0.05$) between plain BC, oxidized BC, or aminated BC for the same pH are marked with *different letters*. **b** Photographs of equal amounts oxidized BC after 10 min centrifugation at 10,000 rpm at pH 4, pH 7, and pH 10 ($n = 3$)

cellulose derived from hardwood. They found that light transmittance, a proxy for dispersibility, increased with increasing carboxyl content from 1.0 to 1.5 mmol/g. According to the findings in Fig. 5, we would expect oxidized BC to have a markedly superior water holding capacity, compared to the other two BC derivatives, due to the increase in surface area.

WRVs of the functionalized BC hydrogels were determined under different pH values to study its swelling behaviour as a function of pH. Oxidized BC was tested from pH 1 (fully protonated and neutral) to pH 10 (deprotonated and charged) and aminated BC was tested from pH 4 (fully protonated and charged) to pH 13 (fully deprotonated and uncharged). In Fig. 6, it can be seen that the WRV of oxidized BC decreases as pH decreases, likely because its charge decreases as pH drops below its pK_a . Likewise, the WRVs of aminated BC decrease as pH increases past the pK_a and the aminated BC becomes neutral, although the result is much less pronounced for aminated BC

compared to oxidized BC. One possible explanation for this is that oxidized BC has a much higher absolute ζ -potential value, thus the interaction with the polar solvent water is much stronger for oxidized BC. Although decreasing the pH of aminated BC from pH 13 increases its surface charge, it also pushes the polymer to a near-zero ζ -potential at pH 7 (Fig. 6a), which would not be a strong driving force for increased water absorption.

Several studies have reported the WRV for PC to be between 50 and 150 % (Saito and Isogai 2004; Saito et al. 2007), significantly less than the value reported here for plain BC of $3,160 \pm 70$ %. This difference can be attributed to the fact that these studies used cellulose from hardwood kraft pulp or cotton linters, which have diameters of 25–50 μm . For a cylindrical fibre, the volume specific surface area is inversely proportional to diameter, and therefore the specific surface area of BC is on the order of 1,000 times that of PC, which explains the almost 100-fold increase in WRV from 50 % for PC to $3,160 \pm 70$ % for BC at pH 7. The high water retention capabilities of plain BC have also been reported elsewhere (Chunyan Zhong 2013; Klemm et al. 2001).

It has been demonstrated in the literature that introduction of carboxyl groups increases the water holding capacity of cellulose derived from hardwood (Saito et al. 2007). With a carboxyl content of 1.5 mmol/g, the WRV value of never-dried TEMPO-oxidized PC was about 400 %, a value approximately 40-times lower than the reported swelling of $16,000 \pm 200$ % for oxidized BC at pH 7 in Fig. 6. At pH 1, the majority of the carboxyl groups on oxidized BC are protonated, whereas at higher pH values, the carboxyl groups were mostly deprotonated (ex. 99 % deprotonated at pH 5.9), thus leading to an expansion between the cellulose fibres due to electrostatic repulsion. This leads to an increased surface area for the hydroxyl and carboxyl groups to interact with water, resulting in greater swelling, with a maximum of $16,800 \pm 200$ % achieved at pH 10.

BC has been investigated for wound healing applications due to its biocompatibility and high water retention. Solway et al. (2011) found that a BC wound dressing is effective for healing of chronic wounds (such as a diabetic foot ulcer) by acting as a scaffold for tissue regeneration. As well, the Brazilian company BioFill Produtos Biotecnologicos has commercialized BC-based wound dressing products. These

products include Biofill[®] and Bioprocess[®], which were used for the treatment of more than 300 ailments, ranging from severe body burns, skin lesions, chronic ulcers, to facial peeling (Czaja et al. 2006). With its higher water holding capacity, oxidized BC may be an improvement as a wound dressing material. It would be superior at maintaining a moist environment, while also being mouldable, mechanically stable and highly absorbable, which are all properties of an ideal wound care dressing (Czaja et al. 2007).

In contrast to the pH-dependent swelling of oxidized BC, the WRV of aminated BC is not as pH-responsive as its anionic counterpart, perhaps because its ζ -potential is closer to zero, which could lead to agglomeration and weaker interaction with the solvent. However, as expected, there is still a trend of increasing swelling with decreasing pH ($R^2 = 0.993$), as the amine group becomes protonated and surface charge increases. However, the changes were not found to be statistically significant ($P > 0.05$). One possible explanation for the lack of stronger pH-dependence is that once the amine groups become protonated, they interact with the anions that give plain BC a negative ζ -potential (Fig. 5), thus reducing electrostatic repulsion and hydrogen bonding to water. This would also cause clumping of the fibres (Fig. 5), and a smaller WRV (Fig. 6).

The maximum change in the average WRV was 350 % for oxidized BC and 28 % for aminated BC. The degree of pH-responsiveness of both samples was superior to the pH response of other natural hydrogels, which was found to be less than 10 % from pH 2.2 to 7.4 (Nkafamiya et al. 2011). However, only the oxidized BC could match the pH response of typical synthetic pH responsive hydrogels which exhibit changes in swelling over up to 300 % (De et al. 2002).

Conclusion

In this study, charged BC derivatives were obtained by the TEMPO-catalyzed oxidation reaction and by the epichlorohydrin-mediated amination reaction. Both the carboxylated BC (pK_a of 3.9 ± 0.1) and the aminated BC (pK_a of 11.0 ± 0.1) are over 99 % charged at physiological pH, making them potential candidates for drug delivery via ionic conjugation of various therapeutic molecules. The oxidized BC derivative showed a marked decrease in its ζ -potential,

while amination caused BC's ζ -potential to increase. The introduction of charges to the BC fibre surface resulted in partial debundling of the fiber bundles leading to a reduction in average fiber diameter. As well, functionalization led to an increase in the water holding capacity of the BC fiber. Since increased water content is a desirable characteristic for the wound-healing environment, these charged BC derivatives could be good wound dressing materials. Moreover, the oxidized BC fibers exhibited a pH dependent water retention property with its WRV increased by fivefold from pH 1 to 7, making it pH responsive hydrogel.

Acknowledgments The authors would like to thank Dr. Richard Gardiner and the UWO Biotron for providing the TEM instruments and guidance with sample preparation. Marko Spaic's work was funded by the Western Graduate Research Scholarship. Darcy Small is the recipient of an NSERC Alexander Graham Bell Scholarship. Justin Cook is the recipient of an NSERC USRA award and CIHR vascular research award.

References

- Bellmann C, Caspari A, Loan Doan T, Mäder E, Luxbacher T, Kohl R (2004) Electrokinetic properties of natural fibres. In: Environmental electrokinetics at the international electrokinetics conference, Pittsburgh, PA
- Benedetti A, Cocco G, Fagherazzi G, Locardi B, Meriani S (1983) X-ray diffraction methods to determine crystallinity and preferred orientation of lithium disilicate in Li–Zn–silicate glass–ceramic fibres. *J Mater Sci* 18(4):1039–1048
- Berg J, Romoser A, Banerjee N, Zebda R, Sayes C (2009) The relationship between pH and zeta potential of ~ 30 nm metal oxide nanoparticle suspensions relevant to in vitro toxicological evaluations. *Nanotoxicology* 3(4):276–283
- Czaja W, Krystynowicz A, Bielecki S, Brown M (2006) Microbial cellulose—the natural power to heal wounds. *Biomaterials* 27(2):145–151
- Czaja W, Young D, Kawecki M, Brown M (2007) The future prospects of microbial cellulose in biomedical applications. *Biomacromolecules* 8(1):1–12
- de Nooy A, Besemer A, van Bekkum H (1995) Highly selective nitroxyl radical-mediated oxidation of primary alcohol groups in water-soluble glucans. *Carbohydr Res* 269(1):89–98
- De S, Aluru N, Johnson B, Crone W, Beebe D, Moore J (2002) Equilibrium swelling and kinetics of pH-responsive hydrogels: models, experiments, and simulations. *J Microelectromech Syst* 11(5):544–555
- De Smedt S, Demeester J, Hennink W (2000) Cationic polymer based gene delivery systems. *Pharm Res* 17(2):113–126
- Decher G (1997) Fuzzy nanoassemblies: toward layered polymeric multicomposites. *Science* 277(5330):1232–1237

- Dong S, Roman M (2007) Fluorescently labeled cellulose nanocrystals for bioimaging applications. *J Am Chem Soc* 129(45):13810–13811
- Fukuzumi H, Saito T, Okita Y, Isogai A (2010) Thermal stabilization of TEMPO-oxidized cellulose. *Polym Degrad Stab* 95(9):1502–1508
- Habibi Y, Lucia L, Rojas O (2010) Cellulose nanocrystals: chemistry, self-assembly, and applications. *Chem Rev* 110(6):3479–3500
- Ifuku S, Tsuji M, Morimoto M, Saimoto H, Yano H (2009) Synthesis of silver nanoparticles templated by TEMPO-mediated oxidized bacterial cellulose nanofibers. *Biomacromolecules* 10(9):2714–2717. doi:10.1021/bm9006979
- Iguchi M, Yamanaka S, Budhiono A (2000) Bacterial cellulose—a masterpiece of nature's arts. *J Mater Sci* 35(2):261–270
- Isogai A, Saito T, Fukuzumi H (2011) TEMPO-oxidized cellulose nanofibers. *Nanoscale* 3(1):71–85
- Kim W, Bonoiu A, Hayakawa T, Xia C, Kakimoto M, Pudavar H, Lee K, Prasad P (2009) Hyperbranched polysiloxysilane nanoparticles: surface charge control of nonviral gene delivery vectors and nanoprobe. *Int J Pharm* 376(1–2):141–152
- Klemm D, Heublein B, Fink H, Bohn A (2005) Cellulose: fascinating biopolymer and sustainable raw material. *Angew Chem Int Ed* 44(22):3358–3393
- Klemm D, Schumann D, Udhardt U, Marsch S (2001) Bacterial synthesized cellulose—artificial blood vessels for microsurgery. *Prog Polym Sci* 26(9):1561–1603
- Klug H, Alexander L (1974) X-ray diffraction procedures for polycrystalline and amorphous materials, 2nd edn. Wiley, New York
- Kötz J, Philipp B, Nehls I, Heinze T, Klemm D (1990) Zum polyelektrolytverhalten einer C-6-substituierten carboxy-cellulose im vergleich zu carboxymethylcellulose. *Acta Polym* 41(6):333–338
- Kumar R, Roy I, Ohulchanskyy T, Goswami L, Bonoiu A, Bergey E, Trampusch K, Maitra A, Prasad P (2008) Covalently dye-linked, surface-controlled, and bioconjugated organically modified silica nanoparticles as targeted probes for optical imaging. *ACS Nano* 2(3):449–456
- Kumar V, Deshpande G (2001) Noncovalent immobilization of bovine serum albumin on oxidized cellulose. *Artif Cell Blood Sub* 29(3):203–212
- Lasseguette E (2008) Grafting onto microfibrils of native cellulose. *Cellulose* 15(4):571–580
- Lee K, Quero F, Blaker J, Hill C, Eichhorn S, Bismarck A (2011) Surface only modification of bacterial cellulose nanofibres with organic acids. *Cellulose* 18(3):595–605
- Liesiene J (2010) Synthesis of water-soluble cationic cellulose derivatives with tertiary amino groups. *Cellulose* 17(1):167–172
- Lokhande H, Salvi A (1978) Electrokinetic studies of cellulosic fibres. *Colloid Polym Sci* 256(10):1021–1026
- Mahmoud K, Mena J, Male K, Hrapovic S, Kamen A, Luong J (2010) Effect of surface charge on the cellular uptake and cytotoxicity of fluorescent labeled cellulose nanocrystals. *ACS Appl Mater Interfaces* 2(10):2924–2932
- Merdan T, Kopecek J, Kissel T (2002) Prospects for cationic polymers in gene and oligonucleotide therapy against cancer. *Adv Drug Deliv Rev* 54(5):715–758
- Millon L, Guhados G, Wan W (2008) Anisotropic polyvinyl alcohol-bacterial cellulose nanocomposite for biomedical applications. *J Biomed Mater Res, Part B* 86B(2):444–452
- Nkafamiya I, Barminas J, Aliyu B, Osemeahon S (2011) Swelling behaviour of konkoli (*Maesopsis eminii*) galactomannan hydrogels. *Int Res J Plant Sci* 2(3):078–086
- Okita Y, Saito T, Isogai A (2010) Entire surface oxidation of various cellulose microfibrils by TEMPO-mediated oxidation. *Biomacromolecules* 11(6):1696–1700
- Patterson A (1939) The Scherrer formula for X-ray particle size determination. *Phys Rev* 56(10):978–982
- Po H, Senozan N (2001) The Henderson–Hasselbalch equation: its history and limitations. *J Chem Educ* 78(11):1499–1503
- Prevey P (1986) The use of Pearson VII distribution functions in X-ray diffraction residual stress measurement. *Adv X Ray Anal* 29:103–111
- Ross P, Mayer R, Benziman M (1991) Cellulose biosynthesis and function in bacteria. *Microbiol Mol Biol Rev* 55(1):35–58
- Saito T, Isogai A (2004) TEMPO-mediated oxidation of native cellulose. The effect of oxidation conditions on chemical and crystal structures of the water-insoluble fractions. *Biomacromolecules* 5(5):1983–1989
- Saito T, Kimura S, Nishiyama Y, Isogai A (2007) Cellulose nanofibers prepared by TEMPO-mediated oxidation of native cellulose. *Biomacromolecules* 8(8):2485–2491
- Saito T, Nishiyama Y, Putaux J, Vignon M, Isogai A (2006a) Homogeneous suspensions of individualized microfibrils from TEMPO-catalyzed oxidation of native cellulose. *Biomacromolecules* 7(6):1687–1691. doi:10.1021/bm060154s
- Saito T, Okita Y, Nge T, Sugiyama J, Isogai A (2006b) TEMPO-mediated oxidation of native cellulose: microscopic analysis of fibrous fractions in the oxidized products. *Carbohydr Polym* 65(4):435–440
- Saito T, Shibata I, Isogai A, Suguri N, Sumikawa N (2005) Distribution of carboxylate groups introduced into cotton linters by the TEMPO-mediated oxidation. *Carbohydr Polym* 61(4):414–419
- Saska S, Barud H, Gaspar A, Marchetto R, Ribeiro S, Messaddeq Y (2011) Bacterial cellulose–hydroxyapatite nanocomposites for bone regeneration. *Int J Biomater* 2011:1–8
- Solway D, Clark W, Levinson D (2011) A parallel open-label trial to evaluate microbial cellulose wound dressing in the treatment of diabetic foot ulcers. *Int Wound J* 8(1):69–73
- Sukhorukov G, Donath E, Lichtenfeld H, Knippel E, Knippel M, Budde A, Mohwald H (1998) Layer-by-layer self assembly of polyelectrolytes on colloidal particles. *Colloid Surf A* 137(1–3):253–266
- Svensson A, Nicklasson E, Harrah T, Panilaitis B, Kaplan D, Brittberg M, Gatenholm P (2005) Bacterial cellulose as a potential scaffold for tissue engineering of cartilage. *Biomaterials* 26(4):419–431
- Wada M, Okano T, Sugiyama J (1997) Synchrotron-radiated X-ray and neutron diffraction study of native cellulose. *Cellulose* 4(3):221–232
- Wan Y, Hong L, Jia S, Huang Y, Zhu Y, Wang Y, Jiang H (2006) Synthesis and characterization of hydroxyapatite–bacterial cellulose nanocomposites. *Compos Sci Technol* 66(11–12):1825–1832

- Wang D, Mohwald H (2004) Template-directed colloidal self-assembly—the route to ‘top-down’ nanochemical engineering. *J Mater Chem* 14(4):459–468
- Weaver J, Armes S, Liu S (2003) A “holy trinity” of micellar aggregates in aqueous solution at ambient temperature: unprecedented self-assembly behavior from a binary mixture of a neutral – cationic diblock copolymer and an anionic polyelectrolyte. *Macromolecules* 36(26):9994–9998
- Wilson A, Prosser H, Powis D (1983) Mechanism of adhesion of polyelectrolyte cements to hydroxyapatite. *J Dent Res* 62(5):590–592
- Yun H, Chen H (2011) Effect of sodium periodate selective oxidation on crystallinity of cotton cellulose. *Adv Mat Res* 197–198:1201–1204
- Zemljic L, Cekara D, Michaelis N, Heinze T, Stana Kleinschek K (2011) Protonation behavior of 6-deoxy-6-(2-aminoethyl)amino cellulose: a potentiometric titration study. *Cellulose* 18(1):33–43. doi:[10.1007/s10570-010-9467-x](https://doi.org/10.1007/s10570-010-9467-x)
- Zhong C (2013) Bacterial cellulose-based ice bags and the production method thereof. US Patent
- Zhu L, Kumar V, Banker G (2001) Examination of oxidized cellulose as a macromolecular prodrug carrier: preparation and characterization of an oxidized cellulose–phenylpropanolamine conjugate. *Int J Pharm* 223(1–2):35–47
- Zhu L, Kumar V, Banker G (2004a) Examination of aqueous oxidized cellulose dispersions as a potential drug carrier: I. Preparation and characterization of oxidized cellulose–phenylpropanolamine complexes. *AAPS PharmSciTech* 5(4):1–7
- Zhu L, Kumar V, Banker G (2004b) Examination of aqueous oxidized cellulose dispersions as a potential drug carrier: II. In vitro and in vivo evaluation of phenylpropanolamine release from microparticles and pellets. *AAPS PharmSci-Tech* 5(4):1–8
- Zimnitsky D, Yurkshtovich T, Bychkovsky P (2006) Adsorption of zwitterionic drugs onto oxidized cellulose. *J Colloid Interface Sci* 295(1):33–40